ELSEVIER

Journal of Nuclear Materials 281 (2000) 34–41

journal of nuclear materials

www.elsevier.nl/locate/jnucmat

Tritium diffusive transport parameters and trapping effects in the reduced activating martensitic steel OPTIFER-IVb

G.A. Esteban *, A. Perujo, K. Douglas, L.A. Sedano [1]

European Commission, Joint Research Center, Environment Institute, T.P. 680, 21020 Ispra (VA), Italy

Received 8 March 2000; accepted 29 May 2000

Abstract

A time-dependent gas-phase isovolumetric desorption technique has been used to obtain the hydrogen isotopes transport parameters between 423 and 892 K and driving pressures ranging from 4×10^4 to 1×10^5 Pa. For protium and deuterium the properties diffusivity (D), Sieverts' constant (K_s), permeability (Φ), trapping energy (E_t) and the trap sites concentration (N_t) are given. On the basis of ideal harmonic vibration of the hydrogen isotope atoms in a unique type of solution site, the values derived for the characteristic protium oscillation temperatures are: $\theta = 1884$ K, $\theta^* = 2387$ K. These values lead to the following extrapolated tritium transport parameters: $D\ (\mathrm{m^2\,s^{-1}}) = 4.166 \times 10^{-8} \exp(-12027/RT)$, $K_s(\mathrm{mol\,m^{-3}\,Pa^{-1/2}}) = 0.271 \exp(-27905/RT)$, $\Phi\ (\mathrm{mol\,m^{-1}\,Pa^{-1/2}\,s^{-1}}) = 1.127 \times 10^{-8} \exp(-39933/RT)$, $E_t\ (\mathrm{J/mol}) = 55554$, and $N_t\ (\mathrm{sites/m^3}) = 0.79 \times 10^{24}$. The dynamics of the hydrogen isotopes transport and the origin of the trapping phenomenon are discussed in connection with the OPTIFER-IVb microstructure.

1. Introduction

Ferritic–martensitic steels are suitable blanket structural materials for thermonuclear fusion devices due to better swelling resistance, lower sensitivity to helium embrittlement and other thermophysical properties [1,2]. OPTIFER-IVb is a CrWVTa martensitic steel optimised to bring together low activating properties with a set of improved mechanical properties, i.e. low ductile-to-brittle transition temperature (DBTT) and a high creep strength [3,4]. This set of properties makes OPTIFER-IVb a quite promising candidate for the design of the blanket structures of the future demonstration reactor (DEMO). Therefore, a complete knowledge of hydrogen (H) isotopes transport parameters is needed in order to evaluate the tritium inventory and permeation through the blanket structure, and also to assess the H-induced embrittlement phenomenon.

H isotopes diffusivity and solubility in steels are strongly affected by trapping at low temperature, from around 573 K and lower (H may be trapped at lattice defect sites such as inclusions, precipitates, grain boundaries or dislocations). Particularly, in this temperature range, trapping may lead to a significant inventory of H trapped in potential energy wells provided by the trapping sites. Moreover, some authors have reported the influence of H trapping on the mechanical behaviour of the steel, accounting for H-induced embrittlement phenomena such as H-induced stress corrosion cracking (HISCC) or cold cracking associated with welding [5]. In relation to this matter a characterisation of trapping is strongly needed.

In the present work, a series of gas/phase isovolumetric desorption experiments (IDE) have been performed for OPTIFER-IVb. The diffusive transport parameters for protium (H_P) and deuterium (H_D): permeability Φ (mol m^{-1} s^{-1} Pa$^{-1/2}$), diffusivity D (m^2 s^{-1}), Sieverts' constant K_s (mol m^{-3} Pa$^{-1/2}$), the density of trap sites N_t (sites/m^3) and the average trapping activation energy E_t (J/mol) are obtained. They have been used

* Corresponding author. Tel.: +39-0332 789 241; fax: +39-0332 785 029.

E-mail address: gustavo.esteban@jrc.it (G.A. Esteban).

[1] Present address: UPV-EHU, ETSIIT, Department of Nuclear Engineering & Fluid Mechanics, Bilbao, Spain.

0022-3115/00/$ - see front matter
PII: S0022-3115(00)00188-4

to evaluate, by extrapolation, the tritium (H_T) diffusive transport parameters.

2. Experimental

The material studied is OPTIFER-IVb [3,4]; a reduced activating martensitic (RAM) 8% CrWVTa steel, heat number 986635, produced by Saarstahl GmbH (Germany). The specimens consisted of four cylinders with a 6 mm diameter and 60 mm height, machined from a rod of material supplied by Forschungszentrum Kalsruhe with the chemical composition (wt%) given in Table 1.

The specimens underwent the following normalising heat treatment: austenising at 1223 K for 0.5 h, fast cooling, tempering at 1003 K for 3 h and finally slow cooling to room temperature. This heat treatment guarantees a fine pre-austenitic grain size, a fully martensitic phase and no pre-eutectoid carbide precipitation. In Fig. 1, the microstructure appearance of the steel can be observed; it shows the well-structured martensite consisting of fine laths.

The surface of the specimens was mechanically polished using a sequence of fine grain SiC abrasive paper and finally with 9, 6 and 3 μm diamond paste. Subsequently the specimens were degreased with acetone and ethanol, then rinsed in distilled water and finally dried in a vacuum furnace before insertion into the experimental rig.

Table 1
Chemical composition of OPTIFER-IVb (wt%)

Element	Concentration (wt%)
C	0.12
Cr	8.3
W	1.4
Mn	0.34
V	0.22
Ta	0.06
N	0.03
Fe	Balance

A schematic view of the isovolumetric desorption installation is shown in Fig. 2. In a conservative manner the experimental values obtained have an error of 5% for the pressure and 1% for the temperature. These errors have been assigned considering the accuracy and stability of the measuring devices and their electronics. They have also been checked by running the same experiment repeatedly.

The technique has been presented in earlier reports [6–9]. Here, we will briefly describe the experimental procedure for clarity. A single isovolumetric desorption run consists of recording the pressure increase in the vessel V1 due to outgassing from the specimen, which has been previously loaded with gas at a given pressure and temperature. During the loading phase a gas concentration in the specimen is built up by diffusion until the equilibrium with external pressure in the specimen is reached. A quick, but thorough pumping down of the vessel V1 breaks this equilibrium between the gas in the sample and the gas in the chamber, starting the gas release from the material. The known volume of the experimental chamber V1 holds the H released from the specimens. The pressure indicates the effective amount of released H and the pressure increase rate the effective H diffusive flux through the specimen surface at every moment of the release phase.

Each measurement is followed by a blank run, under the same experimental conditions (i.e., the same loading pressure and temperature), without specimens, to account for the contribution of the inner wall outgassing of the vessel V1. The 'net' pressure release curve is then obtained by point-to-point pressure subtraction.

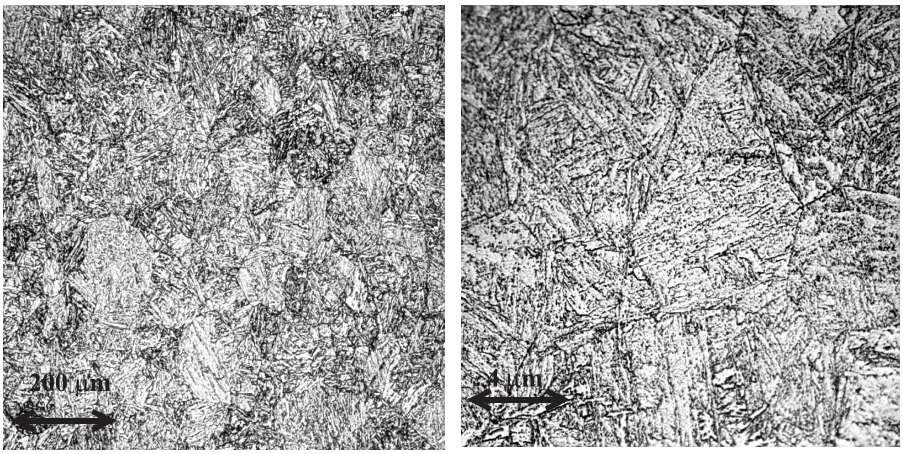

Fig. 1. Optical micrographs of OPTIFER-IVb.

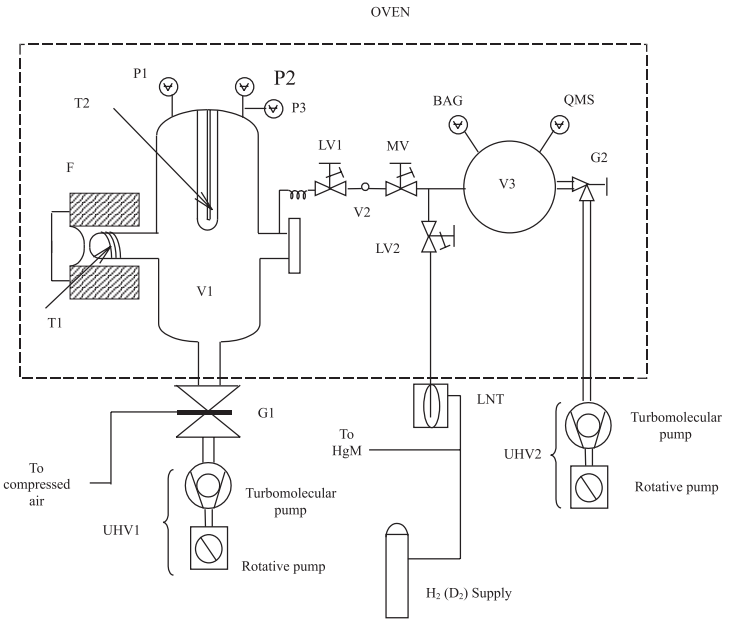

Fig. 2. Schematic view of the measuring facility. BAG – Bayard-Alpert gauge, F – furnace, G1 – electropneumatic gate valve, G2 – manual gate valve, HgM – U-tube Hg manometer, LNT – liquid nitrogen trap, LV1 and LV2 – manual leak valves, MV – manual magnetic valve, P1 and P2 – capacitance manometers, P3 – spinning rotor gauge, QMS – quadrupole mass spectrometer, T1 and T2 Pt – resistance thermometers, UHV – ultra high vacuum pumping units, V1 – experimental chamber, V2 and V3 – expansion volumes.

3. Theory

The effective transport parameters diffusivity D_{eff} and Sieverts' constant $K_{\text{s,eff}}$ are evaluated for each experimental temperature using a non-linear least squares fitting of the theoretical H pressure increase to the experimental increase measured in the experimental chamber V1 (Fig. 3). The permeability Φ is derived from the product of the previous transport parameters, $\Phi = D_{\text{eff}} K_{\text{s,eff}}$, once the diffusive regime has been checked.

The theoretical expression for the pressure increase in the experimental chamber $P(t)$, developed in previous Refs. [6–9] when solving Fick's second law [10], is the following:

$$P(t) = P_{\text{f}} - (P_{\text{f}} + \Delta P) 4 \sum_{n=1}^{\infty} \frac{1}{\alpha_n^2} \exp\left(-\alpha_n^2 \frac{t}{\tau_{\text{d}}} \right), \tag{1}$$

where $P(t)$ is the experimental pressure in the measurement chamber, ΔP is the pressure increase lost during the pump-down period, P_f is the final pressure in the chamber at the end of the release phase, $\tau_{\text{d}} = a^2/D_{\text{eff}}$ (a being the cylinder radius) is the characteristic diffusion time and α_n $(n = 1, 2, \ldots)$ are the infinite real roots of the equation $J_0(\alpha_n) = 0$, $J_0(x)$ being the Bessel function of the first kind and order 0. The effective Sieverts' constant is obtained from ΔP and P_{f} as

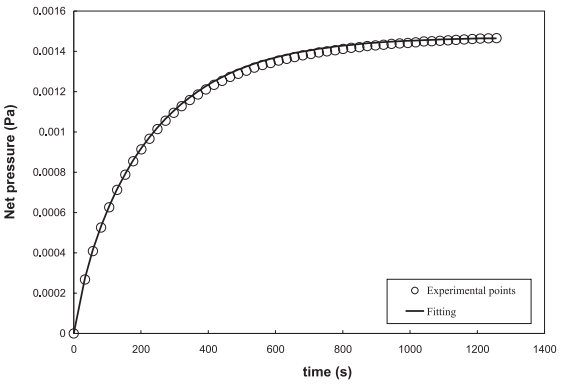

Fig. 3. Experimental pressure increase and fitting.

$$K_{\text{s,eff}} = \frac{(P_{\text{f}} + \Delta P) V1}{V_s R T_{\text{N}}} \left(1 - \sqrt{\frac{P_{\text{f}}}{P_0}} \right)^{-1} P_0^{-1/2}, \tag{2}$$

T_{N} being the normalising temperature, $V1$ the volume of the chamber, V_s the volume of the sample, P_0 the final equilibrium pressure of the loading phase and R the ideal gas constant (8.314 $\text{J K}^{-1}\,\text{mol}^{-1}$).

'Trapping' is the process by which dissolved H atoms remain bound to some specific centres known as 'traps' (e.g., inclusions, dislocations, grain boundaries and precipitates). Hence, hydrogen isotopes may be

dissolved in trapping or lattice sites of the material. The effect of trapping on H transport is, on the one hand, the increase in the gas absorbed inventory, i.e., the increase in the effective Sieverts' constant $K_{s,\mathrm{eff}}$ with respect to the lattice Sieverts' constant K_l; on the other hand, the dynamics of transport becomes slower, i.e., the decrease of the effective diffusivity D_{eff} with respect to the lattice diffusivity D_l:

$$K_{s,l} = K_{s,0} \exp(-E_s/RT), \tag{3}$$

$$K_{s,\mathrm{eff}} = K_{s,l}(1 + (N_t/N_l) \exp(E_t/RT)), \tag{4}$$

$$D_l = D_0 \exp(-E_d/RT), \tag{5}$$

$$D_{\mathrm{eff}} = D_l/(1 + (N_t/N_l) \exp(E_t/RT)). \tag{6}$$

D_0 and K_{s0} being the pre-exponential lattice diffusivity and pre-exponential Sieverts' constant, and E_d and E_s the diffusion and solution energies. N_t (m^{-3}) is the trap sites concentration, N_l (m^{-3}) is the lattice dissolution sites concentration and E_t the trapping energy. Each kind of trap is characterised by a different potential energy, as expressed in Table 2; the potential energy E_t characteristic of the experimented material is the average of all the trapping sites present in that material.

When the effective parameters for each experimental temperature have been obtained, another fitting routine is separately run for the lattice parameters D_0, E_d, K_{s0} and E_s and trapping parameters E_t and N_t over the correspondent temperature range of influence. The value of 5.2×10^{29} sites m^{-3} is taken for the density of solution sites into the lattice N_l, assuming that the martensitic steel is close to a bcc structure, where H occupies only the tetrahedral interstitial positions [20–22].

Table 2
Trapping energies for H in ferritic steels and iron alloys [11–19]

Type of trap	Trapping energy (kJ/mol)	Ref.
Single vacancy	46.6, 50, 78.3	[11,12]
Atomic traps		
Substitutional Cr atoms	26.1	[13]
Substitutional Mo atoms	27	[13]
Substitutional V atoms	27	[13]
Substitutional Mn atoms	10.6	[13]
Substitutional Ni atoms	−11.6	[14]
Interstitial C atoms	3.3	[13]
Interstitial N atoms	12.5	[14]
Grain boundaries	59, 32	[15,16]
Second phase particles (*surfaces*)		
AlN	65	[17]
ε carbide ($Fe_{2-3}C$)	65	[18]
MnS	72	[18]
Dislocations	20–30	[19]

The mass of diffusing gas atoms affects its transport within the material. The theory of harmonic approximation explained in [23–25] is that currently applied to derive tritium transport parameters from H_D and H_P transport data; the usual quantum–statistical partition functions were applied to describe the isotope effect on the solution and diffusion processes [23–26].

4. Results and discussion

As experimental verification of the H atomic dissolution into the steel, OPTIFER-IVb verifies Sieverts' law; i.e., the proportional relation between solubility S (mol m^{-3}) and the square root of the H loading pressure is fulfilled (Fig. 4). The diffusive regime has been confirmed, since diffusivities measured at the same temperature and different pressures overlap without accounting for any surface effect.

The H_P and H_D effective Sieverts' constant and effective diffusivity obtained from modelling the desorption curves are depicted in Figs. 5 and 6 together with the resultant fitting regressions; likewise the derived H_T effective Sieverts' constant and effective diffusivity are depicted. The set of permeabilities is showed in Fig. 7.

The complete set of H_P transport parameters values have been calculated as

$$D\ (\mathrm{m^2\,s^{-1}}) = 5.489 \times 10^{-8} \exp(-10\,574/RT),$$
$$K_s\ (\mathrm{mol\,m^{-3}\,Pa^{-1/2}}) = 0.328 \exp(-29\,005/RT),$$
$$\Phi\ (\mathrm{mol\,m^{-1}\,Pa^{-1/2}\,s^{-1}}) = 1.800 \times 10^{-8} \exp(-39\,579/RT),$$
$$E_t\ (\mathrm{J/mol}) = 52\,169,$$
$$N_t\ (\mathrm{sites/m^3}) = 2.20 \times 10^{24}.$$

The complete set of H_D transport parameters values are

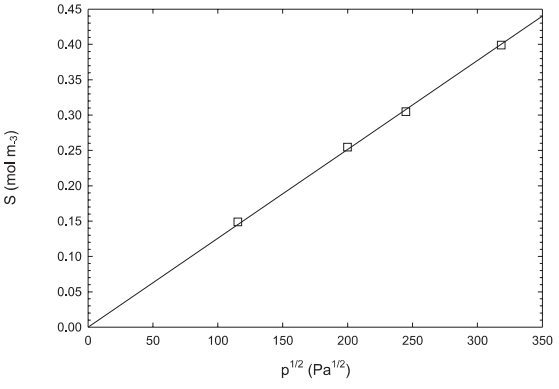

Fig. 4. Solubilities for 630 K at different loading pressures. Sieverts' law confirmed.

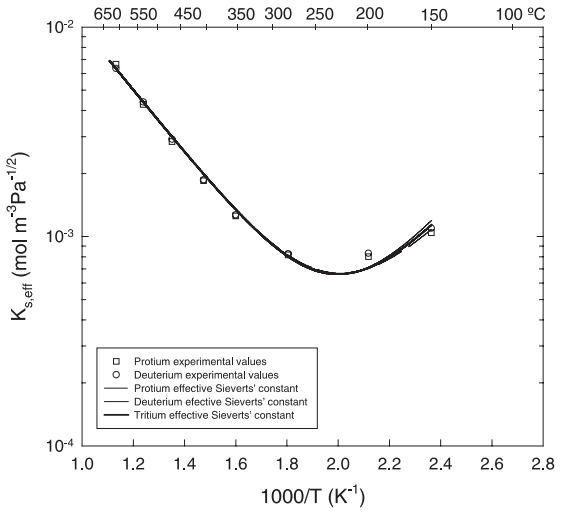

Fig. 5. Arrhenius plot of H isotopes effective Sieverts' constant in OPTIFER-IVb.

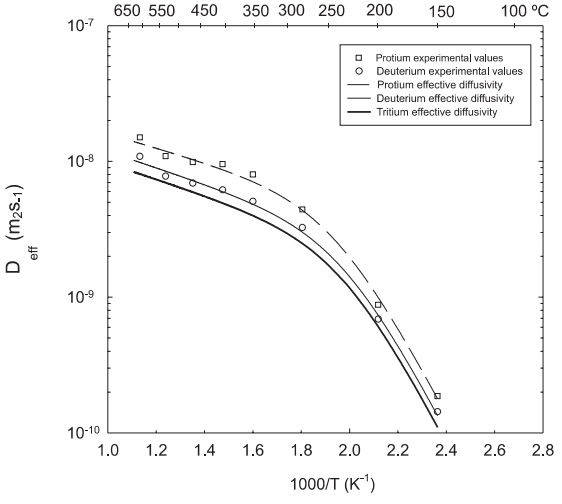

Fig. 6. Arrhenius plot of H isotopes diffusivities in OPTIFER-IVb.

$$D\ (\mathrm{m^2\,s^{-1}}) = 4.613 \times 10^{-8} \exp(-11\,321/RT),$$
$$K_s\ (\mathrm{mol\ m^{-3}\,Pa^{-1/2}}) = 0.325 \exp(-28\,955/RT),$$
$$\Phi\ (\mathrm{mol\ m^{-1}\,Pa^{-1/2}\,s^{-1}}) = 1.500 \times 10^{-8} \exp(-40\,276/RT),$$
$$E_t\ (\mathrm{J/mol}) = 55\,173,$$
$$N_t\ (\mathrm{sites/m^3}) = 1.02 \times 10^{24}.$$

The H_T transport parameters have been inferred from the H_P and H_D transport parameters by applying the extrapolation functions developed in [24–26] with the calculated characteristic protium oscillation temperatures $\theta = 1884$ K, $\theta^* = 2387$ K, and, subsequently, fitted to the Arrhenius expressions:

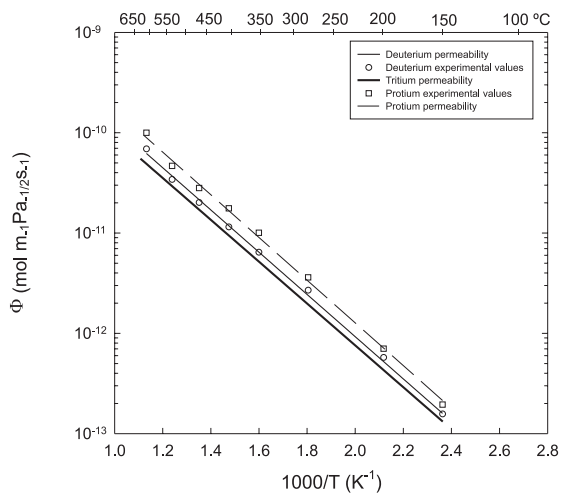

Fig. 7. Arrhenius plot of H isotopes permeabilities in OPTIFER-IVb.

$$D\ (\mathrm{m^2\,s^{-1}}) = 4.166 \times 10^{-8} \exp(-12\,027/RT),$$
$$K_s\ (\mathrm{mol\ m^{-3}\,Pa^{-1/2}}) = 0.271 \exp(-27\,905/RT),$$
$$\Phi\ (\mathrm{mol\ m^{-1}\,Pa^{-1/2}\,s^{-1}}) = 1.127 \times 10^{-8} \exp(-39\,933/RT),$$
$$E_t\ (\mathrm{J/mol}) = 55\,554,$$
$$N_t\ (\mathrm{sites/m^3}) = 0.79 \times 10^{24}.$$

All the isotope diffusive transport parameters are shown in Table 3, together with their respective confidence intervals, the R^2 value (linear fitting quality in obtaining lattice transport parameters) and Pearson's χ^2 (non-linear fitting quality in obtaining trapping parameters).

As expected, OPTIFER-IVb has turned out to be an endothermical absorber of H isotopes. Trapping has been noticed in the low-temperature range (approximately below 573 K). The experimentally obtained trapping energy (52 kJ mol^{-1} for H_P, 55 kJ mol^{-1} for H_D) is close to the trapping energy for high-angle grain boundaries and to those for surfaces of coarse second phase particles (Table 2). Therefore, considering the performed heat treatment and the microstructure of the steel (Fig. 1), it can be proposed, as it was previously for MANET steel [1], that the interfaces between martensitic laths, which represent a type of grain boundary, are the most probable candidates as trapping sites.

It is worth noting that a pre-exponential diffusivities variation amongst the three isotopes is remarkable; for protium and deuterium isotopes the ratio equals 1.19 instead of the classical factor $\sqrt{m_{H_D}/m_{H_P}} = 1.41$, whereas for deuterium and tritium isotopes the ratio is equal to 1.11 instead of the classical factor $\sqrt{m_{H_T}/m_{H_D}} = 1.22$. The differences between the number of trap sites N_t derived for H_P, H_D and H_T are assigned

Table 3
Diffusive transport parameters in OPTIFER-IVb. Confidence intervals and fitting qualities

	Protium	Deuterium	Tritium
D_0 ($\times 10^8$) ($m^2\ s^{-1}$)	5.489 (+0.089, −0.089)	4.613 (+0.098, −0.097)	4.166 (+0.129, −0.129)
E_d (kJ mol^{-1})	10.6 (+0.1, −0.1)	11.3 (+0.1, −0.1)	12.0 (+0.2, −0.2)
R^2	0.8981	0.9428	0.9538
K_{s0} (mol m^{-3} $Pa^{-1/2}$)	0.328 (+0.025, −0.025)	0.325 (+0.026, −0.026)	0.271 (+0.022, −0.022)
E_s (kJ mol^{-1})	29.0 (+0.5, −0.5)	29.0 (+0.5, −0.5)	27.9 (+0.5, −0.5)
R^2	0.9991	0.9996	0.9983
Φ_0 ($\times 10^8$) (mol m^{-1} $Pa^{-1/2}$ s^{-1})	1.800 (+0.189,−0.189)	1.500 (+0.132, −0.132)	1.127 (+0.124, −0.124)
E_Φ (kJ mol^{-1})	39.6(+0.6, −0.5)	40.3 (+0.5, −0.5)	39.9 (+0.6, −0.6)
R^2	0.9983	0.9987	0.9984
N_t ($\times 10^{-24}$) (sites m^{-3})	2.20 (+1.4, −1.4)	1.02 (+0.5, −0.5)	0.79 (+0.5, −0.5)
E_t (kJ mol^{-1})	52.2 (+1.8, −3.6)	55.2 (+1.4, −2.4)	55.6 (+1.8, −3.6)
χ^2	0.110	0.141	0.146

to experimental and statistical errors (the differences are between the confidence intervals) since N_t is a physical property of the material unaffected by the type of diffusing isotope and the stability of the microstructure was assured during both H_P and H_D experimentation. A minor variation has been detected for the Sieverts' constant pre-exponential and for the potential energies (E_s, E_d, E_Φ).

The diffusive transport parameters for OPTIFER-IVb are compared with the results attained for other reference structural steels (Table 4, Figs. 8–10 [2,20,25,27,28]).

The resulting transport parameters for OPTIFER-IVb are consistent with the existing data for other reference martensitic steels. The permeability constant is higher for OPTIFER-IVb than for SS 316L, as is the general behaviour for martensitic steels compared to austenitic. Its diffusion energy is the lowest among all the considered steels whereas the solution energy is close to that of MANET [27]. Moreover, OPTIFER-IVb together with MANET can be referred to as the most endothermic steels among the group.

The trapping energy of OPTIFER-IVb is comparable to the trapping energy of other steels (in the range of MANET [27] and F82H [2]). The same can be stated for the number of trap sites (in the range of Batman [2]).

5. Conclusions

The isovolumetric desorption technique has been undertaken on OPTIFER-IVb, a European candidate martensitic steel manufactured to be employed as a blanket structural material of a future thermonuclear reactor.

The H_P and H_D diffusive transport parameters have been obtained, whereas H_T diffusive transport parameters have been derived by means of quantum-statistical theories. A net reduction on effective diffusivity has been observed in the experiment when changing isotope from H_P to H_D.

The trapping phenomenon is rather pronounced below 573 K, as it has been previously observed for other types of steel. The interfaces between martensitic laths

Table 4
Experimental transport parameters for reference structural steels

Material	K_{s0} (mol m^{-3} $Pa^{-1/2}$)	E_s (kJ mol^{-1})	D_0 ($m^2\ s^{-1}$)	E_d (kJ mol^{-1})	N_t (sites m^{-3})	E_t (kJ mol^{-1})	T (K)	Ref.
OPTIFER-IVb (H_P)	0.328	29.0	5.49×10^8	10.6	2.2×10^{24}	52.2	423–892	TW
OPTIFER-IVb (H_D)	0.325	29.0	4.61×10^8	11.3	1.0×10^{24}	55.2	423–892	TW
OPTIFER-IVb (H_T)	0.271	27.9	4.17×10^8	12.0	7.9×10^{23}	55.5	423–892	TW
MANET (H_P)	0.270	26.7	1.01×10^7	13.2	1.5×10^{25}	48.5	373–743	[27]
MANET (H_P)	0.409	29.6	7.17×10^8	13.5	–	–	523–873	[28]
F82H (H_D)	0.377	26.9	1.07×10^7	13.9	1.6×10^{23}	55.9	373–723	[2]
Batman (H_D)	0.198	24.7	1.90×10^7	15.2	8.6×10^{24}	43.2	373–723	[2]
SS316L (H_P)	1.468	20.6	7.66×10^8	42.5	–	–	523–873	[25]
SS316L (H_P)	0.129	6.9	2.99×10^6	59.7	–	–	600–900	[28]
α-Fe (H_2)	0.510	27.0	3.87×10^8	4.5	4.2×10^{23}	69.0	573–873	[20]

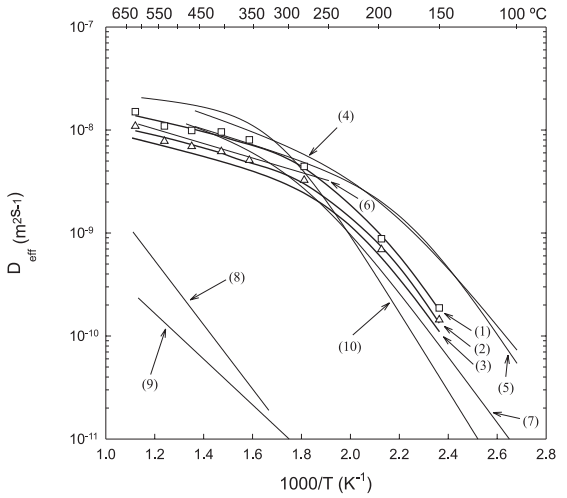

Fig. 8. Diffusivity for OPTIFER-IVb and other reference steels. The squared points are the experimental results for protium, the circled ones are the experimental results for deuterium. (1), (2) and (3), H_P, H_D and H_T, respectively, in OPTIFER-IVb (this work), (4) Batman (H_D) [2], (5) F82H (H_D) [2], (6) MANET (H_P) [27], (7) MANET (H_P) [28], (8) SS 316L (H_P) [28], (9) SS 316L (H_P) [25], (10) α-Fe (H_P) [20].

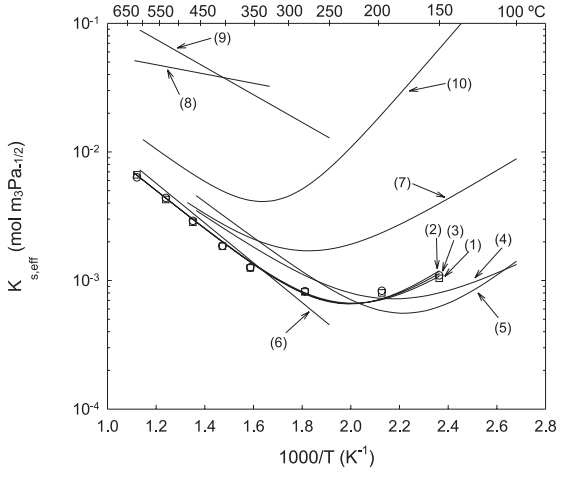

Fig. 9. Sieverts' constant for OPTIFER-IVb and other reference steels. The squared points are the experimental results for protium, the circled ones are the experimental results for deuterium. (1), (2) and (3), H_P, H_D and H_T, respectively, in OPTIFER-IVb (this work), (4) Batman (H_D) [2], (5) F82H (H_D) [2], (6) MANET (H_P) [27], (7) MANET (H_P) [28], (8) SS 316L (H_P) [28], (9) SS 316L (H_P) [25], (10) α-Fe (H_P) [20].

have been identified as the most probable cause of trapping, although the surface of second phase particles are also possible.

This set of transport parameters is consistent with the results obtained for other reference structural martensitic steels showing faster kinetics than austenitic steel. Amongst the martensitic collection, OPTIFER-IVb together with MANET are the most endothermic steels. OPTIFER-IVb has the lowest diffusion energy and its trapping parameters are within the range of the parameters obtained for other martensitic steels.

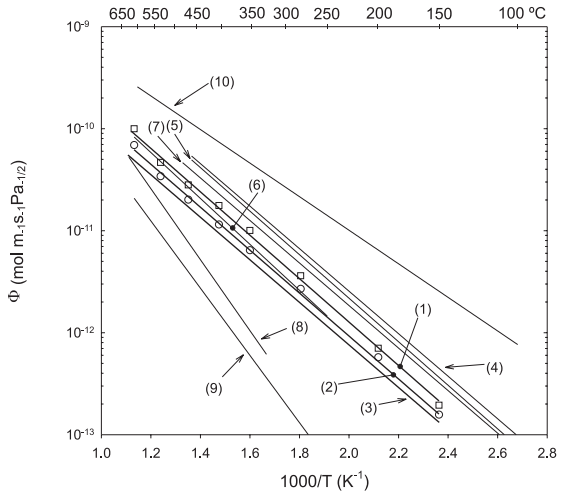

Fig. 10. Permeability for OPTIFER-IVb and other reference steels. The squared points are the experimental results for protium, the circled ones are the experimental results for deuterium. (1), (2) and (3), H_P, H_D and H_T, respectively, in OPTIFER-IVb (this work), (4) Batman (H_D) [2], (5) F82H (H_D) [2], (6) MANET (H_P) [27], (7) MANET (H_P) [28], (8) SS 316L (H_P) [28], (9) SS 316L (H_P) [25], (10) α-Fe (H_P) [20].

References

[1] K.S. Forcey, I. Iordanova, M. Yaneva, J. Nucl. Mater. 240 (1997) 118.
[2] E. Serra, A. Perujo, G. Benamati, J. Nucl. Mater. 245 (1997) 108.
[3] L. Schäfer, M. Schirra, K. Ehrlich, J. Nucl. Mater. 233–237 (1996) 264.
[4] K. Ehrlich, S. Kelzenberg, H.-D. Röhrig, L. Schäfer, M. Schirra, J. Nucl. Mater. 212–215 (1994) 678.
[5] N. Parvathavarthini, S. Saroja, R.K. Dayal, J. Nucl. Mater. 265 (1999) 35.
[6] S. Alberici, A. Perujo, J. Camposilvan, Fus. Technol. 28 (1995) 1108.
[7] L.A Sedano, A. Perujo, Chung H. Wu, J. Nucl. Mater. 273 (1999) p. 285.
[8] S. Tominetti, M. Caorlin, J. Camposilvan, A. Perujo, F. Reiter, J. Nucl. Mater. 176&177 (1990) 672.
[9] G.A. Esteban, L.A. Sedano, A. Perujo, K. Douglas, B. Mancinelli, P.L. Ceroni, G.B. Cueroni, in: Hydrogen Transport Parameters and Trapping Effects in the Martensitic Steel OPTIFER-IVb, EUR 18995 EN, 1999.
[10] H.S. Carslaw, J.C. Jaeger, in: Conduction of Heat in Solids 2nd Ed., Oxford University, New York, 1959.

[11] S.M. Myers, S.T. Picraux, R.E. Stroltz, J. Appl. Phys. 50 (1979) 5710.
[12] K.B. Kimand, S. Pyun, Arch. Eisenhüttenw. 53 (1982) 397.
[13] A.I. Shirley, C.K. Hall, Scr. Metall. 17 (1983) 1003.
[14] J.J. Au, H.K. Birnbaum, Acta Metall. 26 (1978) 1105.
[15] J.R. Scully, J.A. Van Den Avyle, M.J. Cieslak, A.D. Romig Jr., C.R. Hills, Metall. Trans. A 22 (1991) 2429.
[16] J.P. Hirth, Metall. Trans. A 11 (1980) 861.
[17] H.H. Podgurski, R.A. Oriani, Metall. Trans. 3 (1972) 2055.
[18] J. Chene, J.O. García, C.P. de Oliveira, M. Aucouturier, P. Lacombe, J. Microsc. Spectrosc. Electron. 4 (1979) 37.
[19] C.A. Wert, in: G. Alefeld, J. Völkl (Eds.), Topics in Applied Physics, H in Metals II, vol. 29 (1978) p. 305.
[20] K.S. Forcey, I. Iordanova, D.K. Ross, Mater. Sci. Technol. 6 (1990) 357.
[21] K. Kiuchi, R.B. McLellan, Acta Metall. 31 (1983) 961.
[22] A. Seeger, Phys. Lett. A 58 (1976) 137.
[23] Y. Ebisuzaki, W.J. Kass, M. O'Keeffe, J. Chem. Phys. 46 (1967) 1378.
[24] L. Katz, M. Guinan, R.J. Borg, Phys. Rev. B 4 (1971) 330.
[25] F. Reiter, J. Camposilvan, M. Caorlin, G. Saibene, R. Sartori, Fus. Technol. 8 (1985) 2344.
[26] L. Haar, A.S. Friedman, in: Ideal Gas Thermodynamic Functions and Isotope Exchange Functions for the Diatomic Hydrides, Deuterides, and Tritides, US Department of Commerce, National Bureau of Standards, 1961.
[27] E. Serra, A. Perujo, K.S. Forcey, Vuoto 3 (1997) 18.
[28] K.S. Forcey, D.K. Ross, J.C.B. Simpson, J. Nucl. Mater. 160 (1988) 117.